07.2

Features of single-mode emission in 7.5−8.0 μm range quantum-cascade lasers with a short cavity length

© A.V. Babichev[1], E.S. Kolodeznyi[1], A.G. Gladyshev[1], D.V. Denisov[2], N.Yu. Kharin[3], A.D. Petruk[3], V.Yu. Panevin[3], S.O. Slipchenko[4], A.V. Lyutetskii[4], L.Ya. Karachinsky[1,4,5], I.I. Novikov[1,4,5], N.A. Pikhtin[4], A.Yu. Egorov[5]

[1] ITMO University, St. Petersburg, Russia
[2] Petersburg State Electrotechnical University „LETI", St. Petersburg, Russia
[3] Peter the Great Saint-Petersburg Polytechnic University, St. Petersburg, Russia
[4] Ioffe Institute, St. Petersburg, Russia
[5] Connector Optics LLC, St. Petersburg, Russia
E-mail: a.babichev@mail.ioffe.ru

Received October 12, 2021
Revised November 24, 2021
Accepted November 29, 2021

The possibility of realizing single-mode emission in quantum-cascade lasers due to modulation of output optical losses in a Fabry−Perot cavity is demonstrated. For the active region of the 7.5−8.0 μm spectral range, the two-phonon resonance design was used, thus, 50 stages and waveguide layers based on indium phosphide made it possible to realize single-mode 7.765 μm lasing at the temperature of 292 K. Side-mode suppression ratio was about 24 dB and remained the same with an increase in the current pumping up to 1.2 of the threshold current values. The coefficient of wavelength shift with temperature (temperature tuning) in the single-mode lasing regime was 0.56 nm/K.

Keywords: superlattices, quantum-cascade laser, single-mode emission, indium phosphide.

DOI: 10.21883/TPL.2022.03.52872.19050

The conventional approach to realizing single-mode emission in quantum-cascade lasers (QCLs) consists in formation of a diffraction grating in the metallization layers, upper waveguide cladding layers or waveguide side wall [1]. The mode selection can be also achieved by using the photonic crystal design [2], lasers with distributed Bragg reflector [3]. Again, various approaches based on coupled cavities [4–7] make unnecessary the use of relatively complicated methods of electron beam lithography, which is especially hot-topical when no requirements are imposed on the output power but only a narrow-band emission of relatively low power is needed (for instance, for residual gas analyzers). One of the promising approaches proposed in works [8–11] enables the mode selection just due to the presence of a short cavity section.

This paper presents the results of realizing the 7.5−8.0 μm single-mode QCLs in short-cavity stripe lasers.

The QCL heterostructure was epitaxially grown at the commercial molecular−beam epitaxy facility Riber 49 at „Connector Optics" LLC. Prior to growing the active region layers on the InP (001) substrate with the doping level of $(1-3)\cdot 10^{17}\,\mathrm{cm}^{-3}$, an $In_{0.53}Ga_{0.47}As$ buffer layer 500 nm thick with the doping level of $5\cdot 10^{16}\,\mathrm{cm}^{-3}$ was formed. In creating the 7.5−8.0 μm active region, the two-phonon resonance design was used. The active region comprised 50 stages forming the cascade [12]. The top waveguide cladding comprised an indium phosphide layer 3.9 μm thick with the doping level of $1\cdot 10^{17}\,\mathrm{cm}^{-3}$. Contact layers based on $In_{0.53}Ga_{0.47}As$ with the thicknesses of 100 and 20 nm and doping levels of $1\cdot 10^{17}$ and $1\cdot 10^{19}\,\mathrm{cm}^{-3}$ were used for current injection. The stripe laser mesa was formed by liquid etching with subsequent application of dielectric and metallization layers. The stripe contact width was 50 μm. The Fabry−Perot cavity mirrors 210 μm long were formed by hand cleaving after thinning the substrate. The QCL crystals were mounted on a copper heatsink with the epitaxial surface down [12].

The Fig. 1, *a* inset presents the dependence of the intermode interval (free spectral range, FSR) on the stripe laser cavity length; this dependence is defined as $\nu_{\mathrm{FSR}} = 2n_{gr}L$, where n_{gr} is the group refractive index, L is the laser cavity length. It was shown that, when the cavity length is about 200 μm, typical values of ν_{FSR} are $\sim 7\,\mathrm{cm}^{-1}$. For the laser design under study, the gain margin ratio (GMR) characterizing the ratio between the peak gain factor and gain factor corresponding to the position of the nearest side optical mode is 1.03 (if the spontaneous emission spectrum is approximated with the Lorenz function [11]). Hence, in the experiment with the stripe laser length of about 200 μm it is possible to perform efficient selection of longitudinal optical modes and realize the single-mode emission regime.

The emission spectra were measured with a Fourier spectrometer Bruker Vertex 80v. For the signal detection in the step-scan mode, a fast-response HgCdTe photodiode cooled to the liquid nitrogen boiling point was used; the typical response time of the photodiode was ∼ 100 ns. Analysis of the laser spectral characteristics and of the emission pulse intensity dependence on the current pumping

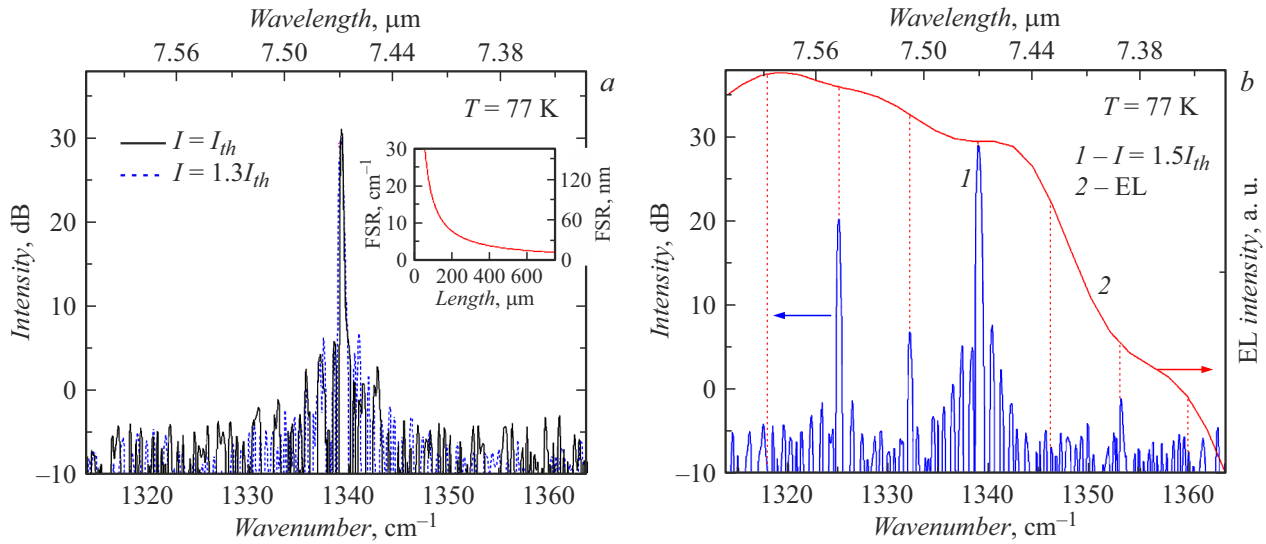

Figure 1. Emission spectra of the QCL under study measured at 77 K. *a* — at the threshold current I_{th} (solid line) and at $1.3I_{th}$ (dashed line); *b* — at $1.5I_{th}$ (*1*); the spontaneous emission spectrum is also presented in the semi-logarithmic scale [13] (*2*). The inset (panel *a*) presents the intermode interval versus the Fabry–Perot cavity length.

level gave the current pumping pulse length of 100 and 70 ns, respectively. The pulse repetition rate was 15 kHz in both experiments. The measurements were performed at temperatures T equal to 77 and 292 K.

Fig. 1 presents the emission spectra of a stripe QCL with the cavity length of 210 μm; the measurement temperature was 77 K. At the pumping current close to the threshold (I_{th}) there was observed the 7.467 μm single-mode emission with the side-mode suppression ratio (SMSR) of about 25 dB (Fig. 1, *a*). The emission line FWHM was shown to be as low as ~ 1.4 nm. The increase in the pumping current results in emergence of extra optical modes with the wavelengths of $\lambda = 7.547\,\mu$m (at $1.41I_{th}$) and $\lambda = 7.507$, $7.387\,\mu$m (at $1.5I_{th}$, Fig. 1, *b*). The intermode interval $\nu_{\mathrm{FSR}} = 7.2\,\mathrm{cm}^{-1}$ ($\lambda_{\mathrm{FSR}} = 40$ nm) indicated in Fig. 1, *b* with vertical dashed lines corresponds to the group refractive index $n_{gr} = 3.3$. Fig. 1, *b* presents also the spontaneous emission spectrum [13]. The GMR estimate obtained by analyzing the spontaneous emission spectrum was 1.02. The coefficient of the emission wavelength shift with increasing pumping current $\Delta\lambda/\Delta I$ was ~ 5 nm/A. No decrease in the emission integral intensity was observed while the pumping current increased to $1.5I_{th}$. Thus, in the pumping current range from the threshold to $1.36I_{th}$, the single-mode emission with SMSR $\geqslant 24$ dB is observed at $T = 77$ K. Further increase in the pumping current results in emergence of additional spectral lines and decrease in the SMSR ratio. At 77 K, the threshold current density j_{th} of the laser appeared to be 4.2 kA/cm^2. The increase in the laser temperature to 292 K results in the j_{th} increase to 9.9 kA/cm^2. Fig. 2 demonstrates the dependence of the emission pulse intensity on the pumping current (corresponding to the temperature of 292 K). Using relation $j_{th}(T) = j_0 \exp(T/T_0)$, where j_0 is the threshold current density at zero temperature, the

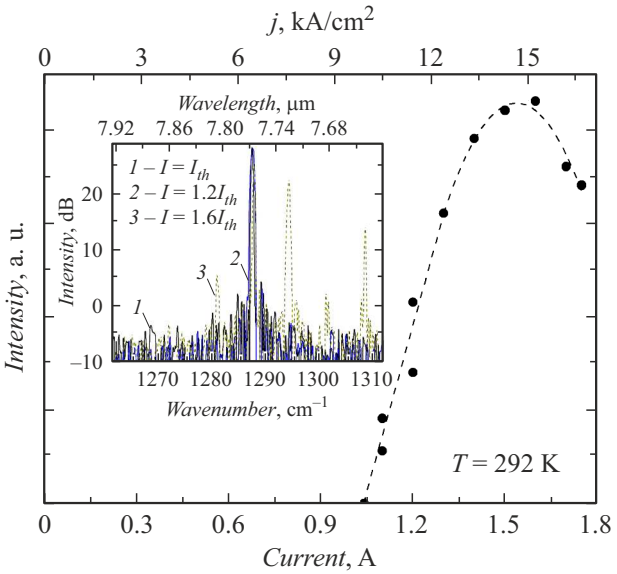

Figure 2. The emission pulse intensity versus the current pumping level. The inset presents the emission spectra measured at 292 K at different pumping currents.

characteristic temperature of the threshold current stability T_0 was estimated. The T_0 and j_0 values were 250 K and 3.1 kA/cm^2, respectively.

The emission spectra measured at 292 K are presented in the Fig. 2 inset. Near the threshold, the single-mode emission at 7.765 μm is observed. The presence of single-mode emission with SMSR $\geqslant 24$ dB is shown for the pumping current range from the threshold to $1.2I_{th}$. Further increase in the pumping level leads to the emergence of optical modes with wavelengths $\lambda = 7.724\,\mu$m (at $1.24I_{th}$)

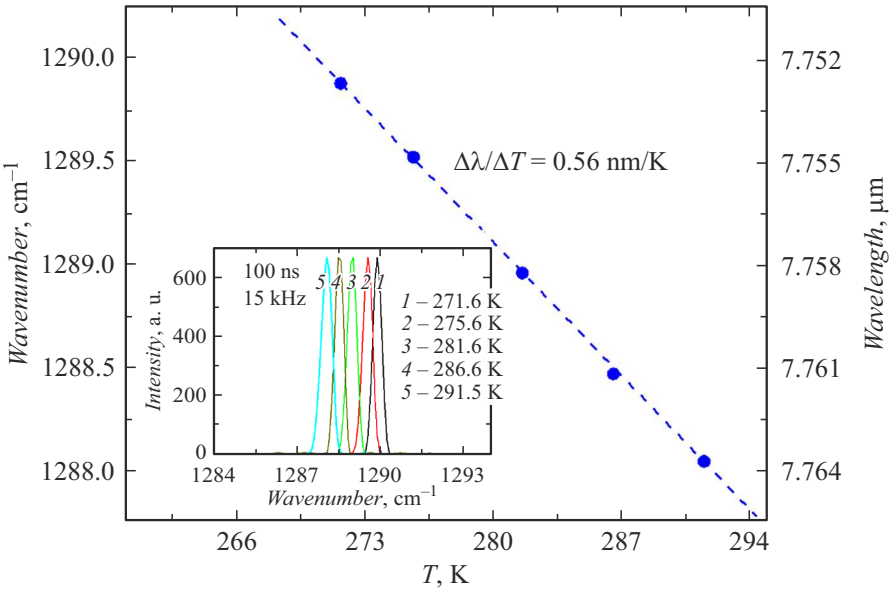

Figure 3. The emission wavelength (single-mode regime) versus temperature. The pumping current is fixed at $1.01I_{th}$. The inset demonstrates standardized spectra of single-mode emission measured at different temperatures.

and $\lambda = 7.644\,\mu$m (at $1.26I_{th}$). The emission spectrum measured at $1.6I_{th}$ is represented by four optical modes close to 7.762, 7.724, 7.644 and 7.601 μm. Taking into account the known intermode interval, estimates of the laser mirror refractive index (0.29) and output optical losses ($13\,\text{cm}^{-1}$) were obtained.

The samples under study exhibited continuous temperature tuning of the emission wavelength in the single-mode emission regime (Fig. 3). A long-wave shift of the emission wavelength with increasing temperature was demonstrated. Earlier it was assumed [14] that, along with the Stark effect, reduction of the conductive band offset (CBO) may be a source of the emission wavelength long-wave shift with the temperature increase. The numerical estimation showed that there are two stages of the CBO variation with temperature for the studied heteropair $In_{0.53}Ga_{0.47}As/In_{0.52}Al_{0.48}As$. In the temperature range of 77–150 K, a CBO increase with increasing temperature is observed. Further the temperature increase leads to a drop in CBO. During the temperature increase from 77 to 292 K, the CBO value decreases from 527 to 523 meV, which agrees well with the experiment (long-wave shift of the emission wavelength from 7.467 to 7.765 μm with the temperature increase from77 to 292 K).

The threshold voltage U_{th} was estimated at different temperatures. The minimal U_{th} (~ 12.4 V) corresponds to ~ 150 K. When the temperature increases to 292 K, the U_{th} increase to ~ 15.0 V is observed, which is caused by the effect of above-barrier carrier emission into the continuous spectrum [14]. The mentioned threshold voltage increase with increasing temperature due to the Stark quantum effect is expected to initiate the short-wave shift of the emission wavelength. However, contrary to the results of [14], it is possible that the Stark quantum effect does not dominate because of the „off–diagonal“ active region design used in this work.

Based on the single-mode emission spectra measured at different temperatures (see the Fig. 3 inset), the coefficient of the wavelength shift with temperature in the single-mode emission regime ($\Delta\lambda/\Delta T$) was estimated. The $\Delta\lambda/\Delta T$ value was $+0.56$ nm/K ($-0.09\,\text{cm}^{-1}$/K), which matches with the earlier obtained results for single-mode QCLs of the 7.5–8.5 μm (0.53–0.58 nm/K) spectral range [15,16].

In summary, notice that the reported study resulted in creating the 7.5–8.0 μm single-mode QCLs and revealing their characteristics. Reduction of the cavity length to 210 μm results in an increase in the intermode interval to 40 nm and also in an increase in GMR that characterizes the ratio between the peak gain factor and gain factor corresponding to the position of the stripe laser nearest side mode; this enables realization of the single-mode emission with the side-mode suppression ratio of 24 dB at 292 K within the pumping current range from the threshold to $1.2I_{th}$. The coefficient of wavelength shift with temperature (temperature tuning) was 0.56 nm/K.

Financial support

The study was supported by the Russian Scientific Foundation (project № 20-79-10285).

Conflict of interests

The authors declare that they have no conflict of interests.

References

[1] J. Faist, C. Gmachl, F. Capasso, C. Sirtori, D.L. Sivco, J.N. Baillargeon, A.Y. Cho, Appl. Phys. Lett., **70** (20), 2670 (1997). DOI: 10.1063/1.119208

[2] Z. Wang, Y. Liang, B. Meng, Y.-T. Sun, G. Omanakuttan, E. Gini, M. Beck, I. Sergachev, S. Lourdudoss, J. Faist, G. Scalari, Opt. Express, **27** (16), 22708 (2019). DOI: 10.1364/oe.27.022708

[3] A. Sadeghi, P.Q. Liu, X. Wang, J. Fan, M. Troccoli, C.F. Gmachl, Opt. Express, **21** (25), 31012 (2013). DOI: 10.1364/OE.21.031012

[4] P.Q. Liu, X. Wang, C.F. Gmachl, Appl. Phys. Lett., **101** (16), 161115 (2012). DOI: 10.1063/1.4761247

[5] H. Knötig, B. Hinkov, R. Weih, S. Höfling, J. Koeth, G. Strasser, Appl. Phys. Lett., **116** (13), 131101 (2020). DOI: 10.1063/1.5139649

[6] Y. Wakayama, S. Iwamoto, Y. Arakawa, Appl. Phys. Lett., **96** (17), 171104 (2010). DOI: 10.1063/1.3413949

[7] M.C. Zheng, N.L. Aung, A. Basak, P.Q. Liu, X. Wang, J.-Y. Fan, M. Troccoli, C.F. Gmachl, Opt. Express, **23** (3), 2713 (2015). DOI: 10.1364/oe.23.002713

[8] B. Schwarz, C.A. Wang, L. Missaggia, T.S. Mansuripur, P. Chevalier, M.K. Connors, D. McNulty, J. Cederberg, G. Strasser, F. Capasso, ACS Photonics, **4** (5), 1225 (2017). DOI: 10.1021/acsphotonics.7b00133

[9] I. Kundu, J.R. Freeman, P. Dean, L. Li, E.H. Linfield, A.G. Davies, ACS Photonics, **7** (3), 765 (2020). DOI: 10.1021/acsphotonics.9b01616

[10] K. Pierściński, D. Pierścińska, A. Kuźmicz, G. Sobczak, M. Bugajski, P. Gutowski, K. Chmielewski, Photonics, **7** (3), 45 (2020). DOI: 10.3390/photonics7030045

[11] R.A. Cendejas, Z. Liu, W. Sánchez-Vaynshteyn, C.G. Caneau, C.-E. Zah, C. Gmachl, IEEE Photonics J., **3** (1), 71 (2011). DOI: 10.1109/JPHOT.2010.2103376

[12] A.V. Babichev, A.G. Gladyshev, A.S. Kurochkin, V.V. Dudelev, E.S. Kolodeznyi, G.S. Sokolovskii, V.E. Bugrov, L.Ya. Karachinsky, I.I. Novikov, D.V. Denisov, A.S. Ionov, S.O. Slipchenko, A.V. Lyutetskii, N.A. Pikhtin, A.Yu. Egorov, Tech. Phys. Lett., **45** (4), 398 (2019). DOI: 10.1134/s1063785019040205.

[13] A.V. Babichev, A.G. Gladyshev, E.S. Kolodeznyi, A.S. Kurochkin, G.S. Sokolovskii, V.E. Bougrov, L.Ya. Karachinsky, I.I. Novikov, V.V. Dudelev, V.N. Nevedomsky, S.O. Slipchenko, A.V. Lutetskiy, A.N. Sofronov, D.A. Firsov, L.E. Vorobjev, N.A. Pikhtin, A.Yu. Egorov, J. Phys.: Conf. Ser., **1124** (4), 041029 (2018). DOI: 10.1088/1742-6596/1124/4/041029

[14] Y. Bai, S. Slivken, S. Kuboya, S.R. Darvish, M. Razeghi, Nat. Photonics, **4** (2), 99 (2010). DOI: 10.1038/nphoton.2009.263

[15] J. Faist, C. Gmachl, F. Capasso, C. Sirtori, D.L. Sivco, J.N. Baillargeon, A.Y. Cho, Appl. Phys. Lett., **70** (20), 2670 (1997). DOI: 10.1063/1.119208

[16] C. Gmachl, F. Capasso, J. Faist, A.L. Hutchinson, A. Tredicucci, D.L. Sivco, J.N. Baillargeon, S.N.G. Chu, A.Y. Cho, Appl. Phys. Lett., **72** (12), 1430 (1998). DOI: 10.1063/1.120585